Hydrogels with Cell Adhesion Peptide-Decorated Channel Walls for Cell Guidance

Shuang Wang, Mariah Sarwat, Peng Wang, Denver C. Surrao, Damien G. Harkin, James A. St John, Eleonore C. L. Bolle, Aurelien Forget, Paul D. Dalton,* and Tim R. Dargaville*

A method is reported for making hollow channels within hydrogels decorated with cell-adhesion peptides exclusively at the channel surface. Sacrificial fibers of different diameters are used to introduce channels within poly(ethylene glycol) hydrogels crosslinked with maleimide-thiol chemistry, which are back-filled with a cysteine-containing peptide solution which is conjugated to the lumen with good spatial efficiency. This allows for peptide patterning in only the areas of the hydrogel where they are needed when used as cell-guides, reducing the amount of required peptide 20-fold when compared to bulk functionalization. The power of this approach is highlighted by successfully using these patterned hydrogels without active perfusion to guide fibroblasts and olfactory ensheathing cells—the latter having unique potential in neural repair therapies.

Hydrogels containing channels capable of guiding cell growth are of particular interest for tissue engineering applications where alignment of cells is critical to function, such as neural regeneration applications.[1–6] The use of sacrificial molding

S. Wang, M. Sarwat, P. Wang, Prof. D. G. Harkin, Dr. E. C. L. Bolle, Prof. T. R. Dargaville
Institute of Health and Biomedical Innovation
Queensland University of Technology
60 Musk Avenue, Kelvin Grove, Queensland 4059, Australia
E-mail: t.dargaville@qut.edu.au

Dr. D. C. Surrao, Prof. J. A. St John
Clem Jones Centre for Neurobiology and Stem Cell Research and Griffith University for Drug Discovery
Griffith University
Brisbane, Queensland 4111, Australia

Dr. A. Forget
Institute for Macromolecular Chemistry
University of Freiburg
Stefan-Meier-Str. 31, Freiburg 79104, Germany

Prof. P. D. Dalton
Department for Functional Materials in Medicine and Dentistry and Bavarian Polymer Institute
University Clinic Würzburg
Pleicherwall 2, Würzburg D97070, Germany
E-mail: paul.dalton@fmz.uni-wuerzburg.de

The ORCID identification number(s) for the author(s) of this article can be found under https://doi.org/10.1002/marc.202000295.

with additively manufactured templates is an appealing approach to make hollow channels whereby defined architectures can be translated to the porous features within the hydrogels.[4,7,8] In this method, the hydrogel precursor solution is cast around the template and allowed to gel before removing the template, which is accomplished by various techniques, including dissolution,[9–11] aspiration by manual pulling or by vacuum,[12] and lique-faction upon heating.[13–15] These methods work well with hydrogels containing native cell adhesion sites throughout their polymer backbone, such as collagen and gelatin. However, the desirable physical complexity of the channeled hydrogels is somewhat negated by the lack of control over the chemistry between the bulk hydrogel and the luminal walls. For synthetic hydrogels, this often results in the channels being void of the haptotactic signals found in native extracellular matrix (ECM).[16]

An alternative to sacrificial molding is photo-immobilization where spatially distinct immobilization of biomolecules, in this case cell adhesion peptides (CAPs), is achieved. With this technique columns of peptides within synthetic hydrogels have been reported, however, this requires infusion of the whole gel with the peptides followed by subsequent extraction of non-bound peptide even though only a small fraction of the matrix is modified.[3] Depending on the hydrogel volume, the quantity of CAP required can become significant and costly, especially with longer peptide sequences. Simply reducing the hydrogel volume is one solution (e.g., via hydrogel microarrays[17]), however specialized equipment is required, and handling limitations can outweigh the benefits unless very high-throughput experiments are the goal.[18]

Our aim in this study is to overcome these two challenges, namely, to pattern hydrogels with channels of pre-determined diameters where the channel walls are selectively functionalized with CAPs. Recently, we introduced a method for spatially patterning hydrogels using a 3D stamping technique with a dissolvable ink, ideally using hydrophobic molecules for transfer.[19] However, we subsequently discovered an even simpler approach for patterning hydrophilic molecules, including CAPs, which requires substantially lower peptide quantities. Here, we present a general strategy to generate patterned channels with a range of dimensions to support cell growth

4-arm PEG Maleimide (PEG-4Mal), M_w =20,000   4-arm PEG thiol (PEG-4SH), M_w =5,000
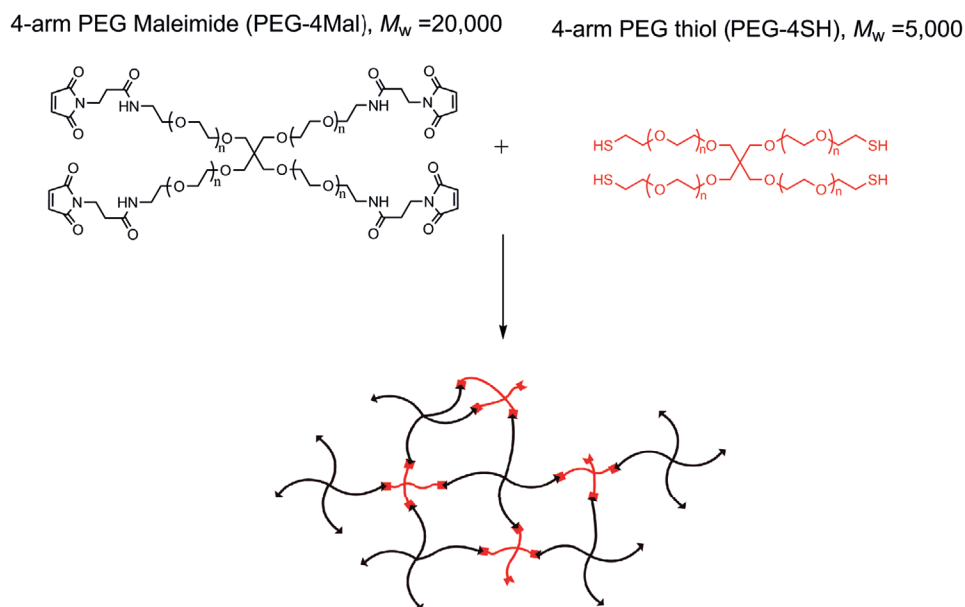
Scheme 1. PEG-4Mal crosslinked with PEG-4SH via thiol-Michael addition reaction.

without active perfusion. Two additive manufacturing processes, namely fused deposition modelling (FDM) and melt electrowriting (MEW) were used to create channel templates with a large range of diameters within poly(ethylene glycol) (PEG) hydrogels. The channels were subsequently conjugated with a CAP using a fluid flow method, and seeded with either NIH-3T3 fibroblasts or mouse olfactory ensheathing cells (mOECs), the latter being a cell transplantation candidate for treating spinal cord injuries.[20] The optimization of conjugation chemistry, efficiency of the peptide usage, the ease of control over the sizes of the channels, the flexibility of the dose and distribution of the peptides, as well as cell response to the patterned channels are presented.

Fused deposition modeling (FDM), was used to extrude PCL filament with diameters ranging from 170 to 530 μm by varying the nozzle travel speed (Figure S1a, Supporting Information) while melt electrowriting (MEW)[21–27] was used to produce a range of fibers with diameters from 50 to 220 μm (Figure S1b, Supporting Information). Thus, by using both FDM and MEW uniform multiscale filaments and fibers of PCL ranging from 50 to 500 μm could be fabricated as channel templates for the hydrogels.

The hydrogels used in this study were synthesized from a combination of two 4-arm PEG precursors with Michael-type reactive end-groups, namely, PEG-maleimide (PEG-4Mal) and PEG-thiol (PEG-4SH). This PEG-maleimide-thiol combination has been used extensively to make hydrogels[28,29] and has the flexibility to rapidly covalently-bind peptides bearing cysteine residues where the thiol group of the cysteine can react with PEG-maleimide groups. Usually though, the peptide is incorporated either before or during gelation, however for the purposes of this study the peptide required conjugation after hydrogel formation. To achieve this an off-stoichiometric ratio of PEG-4Mal and PEG-4SH was used so that free maleimide residues would be present after gelation (**Scheme 1**). At 0.5

molar excess of PEG-4Mal the theoretical concentrations of the unreacted maleimide groups in 5%, 10%, and 15% w/v hydrogels were 2.9, 5.7, and 8.6 mм, respectively.

The gelation time at pH 7.3 was too rapid to effectively handle the hydrogels, but by using a lower pH (pH 4) the reaction kinetics were slowed due to lower concentration of reactive thiolate anions, to allow for gelation time of 30–120 s, depending on solid content. The obtained hydrogels were transparent and the swelling properties and Young's moduli correlated well with solid content (Table S1, Supporting Information). All hydrogels had stiffness above the ca. 1.2 kPa threshold for cells to migrate through.[30]

To create channels within the hydrogels, the PEG precursors were cast around PCL filaments and fibers. Once the hydrogels had fully cured and reached equilibrium swelling, the PCL was removed either by manual physical extraction (Figure S2, Supporting Information) or by using 90% acetone with gentle sonication to dissolve nonlinear 2D and 3D templates. The removal process yielded channels with high fidelity and diameters that were ≈1.5 times the size of the template fibers due to swelling of the hydrogels after curing.

To selectively pattern the channel walls created by the channels with CAPs, a solution of CRGDSGK (with 10% of the peptide tagged with fluorescein for visualization) was injected through the channels using a syringe tip at the channel inlet. After 30 min post-injection, fluorescence microscopy was used to confirm that the peptide was immobilized along the entire channel (Figure S3, Supporting Information). To measure the efficiency of the process the unreacted peptide solutions retrieved from the channels were analyzed for fluorescence intensity and thiol content (via Ellman's assay) which indicated that less than 1% of the initial amount of peptide remained unreacted (Figure S4, Supporting Information), suggesting approximately 99% efficiency in conjugation of the peptide to the hydrogel.
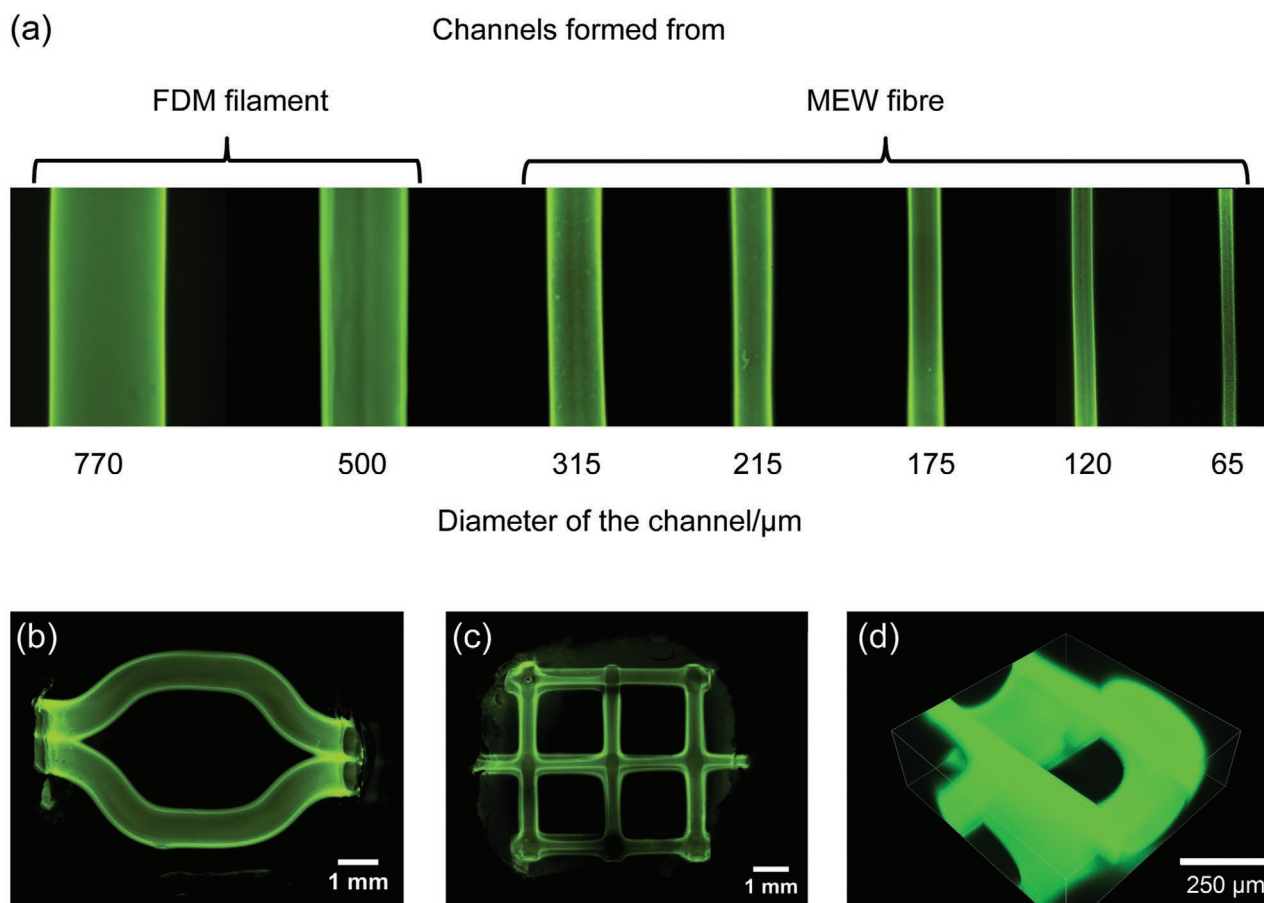
**ADVANCED
SCIENCE NEWS**
www.advancedsciencenews.com

**Macromolecular
Rapid Communications**
www.mrc-journal.de

Figure 1. a) Fluorescence stereomicroscope images of straight patterned channels with different sizes created using FDM and MEW, b) a 2D pattern, c) a 3D pattern, and d) z-stack confocal laser scanning microscope (CLSM) image of two interconnected channels from the 3D pattern.

The mechanism of patterning is governed by both chemical and physical processes. The chemical process is the Michael-type conjugation reaction between the thiol on the cysteine residue of the peptide and the maleimide groups on the polymer; whereas the physical process is the diffusion of the peptide from within the channels to the surrounding hydrogel. If the conjugation reaction is slow relative to diffusion then the peptide becomes smeared throughout the hydrogel as is the case when the less reactive PEG-vinyl sulfone is used instead of PEG-4Mal (results not shown). Thus, the success of this method relies strongly on the high reactivity of the PEG-4Mal to thiols at the correct pH.

To determine the precision of the injection method, the hydrogels were imaged using fluorescence microscopy after CAP immobilization. **Figure 1**a shows well-defined patterned channels with diameters ranging from 64 to 770 µm by using PCL FDM filaments and MEW fibers. As proof-of-principal, more complex templates were used to create curved and multi-layer interconnected channels which were functionalized with the peptide with high fidelity (Figure 1b–d).

To quantify the penetration depth of the peptide, the distance from the channel to where the fluorescence intensity was an arbitrary 50% of the maximum was measured

(**Figure 2**). Due to the lowest crosslinking density, the 5% gel had the longest penetration distance of 138 ± 6 µm, while in the 10% and 15% gels the peptide penetrated shorter distances (103 ± 4 and 93 ± 8 µm, respectively). Decreasing the concentration of the peptide mixture resulted in a migration distance of 17 ± 2 µm due to rapid consumption of the peptide. For 10% gels, the concentrations of the peptide at the interface of channels patterned with 1 and 0.1 mM peptide mixtures were ≈2 and 0.2 mM, respectively (Equation S1, Supporting Information).

To investigate the peptide-functionalized channels as cell guides, NIH-3T3 cells were initially chosen to establish: i) that cells could indeed be seeded into the channels, ii) that the cells would remain in the channels and not migrate into the bulk hydrogels, and iii) that the concentration of peptide was relevant. The effect of peptide concentration was investigated by culturing NIH-3T3 cells in the 10% w/v hydrogel channels conjugated with either 0.2 or 2 mM of peptide solution and with no peptide as control (Figure S5, Supporting Information). In the control group, NIH-3T3 cells showed a rounded morphology as expected for PEG hydrogels lacking cell adhesion motifs,[30] while the 0.2 mM peptide concentration facilitated limited, but improved, cell adhesion and proliferation. Using a
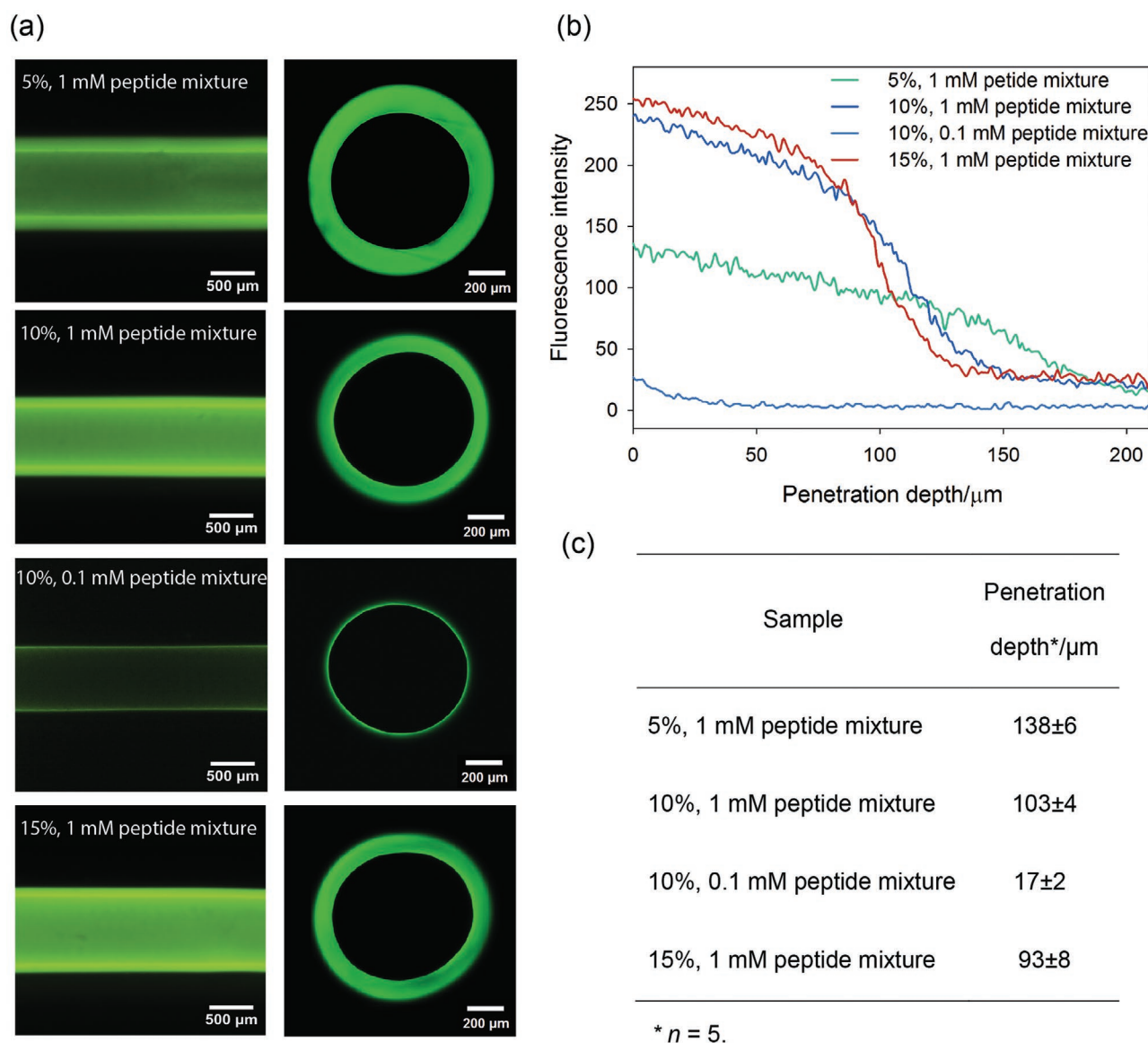
2000295 (3 of 7)

Figure 2. a) Fluorescence microscopy images from above and confocal images of the cross-section of the patterned channels (10×) with different solid contents and injected peptide mixture concentrations after thorough washing of the non-bound molecules, b) gradient intensity profile of the patterned channels, and c) penetration depth measured as the full width at half maximum.

peptide concentration of 2 mM further improved cell adhesion and growth, indicating sufficient concentration of the integrin binding motif on the channel wall. Importantly, the NIH-3T3 cells only attached and proliferated on the channel walls without invading into the bulk hydrogel, even when the peptide was functionalized through the bulk hydrogel (Figure S6, Supporting Information).

The channel patterning method greatly reduced the total amount of peptide needed compared with hydrogels with the peptide distributed throughout. For the 30 μL hydrogels with a single 600 μm diameter channel, conjugating 2 mM peptide throughout the hydrogel required 60 nmol of peptide; while with the perfusion method only 3 nmol was needed—a 20-fold reduction in peptide amount.

After initial screening with NIH-3T3 cells, mOECs were seeded into the channels. Such glial cells are known to aid in axonal guidance and have been researched as a cell transplantation candidate to treat spinal cord injury.[1,20] Organisation of mOEC into linear structures is highly valuable to mimic their behavior after transplantation. Channels with diameters of 600, 300, and 150 μm with and without peptide patterning were used with 1 mM peptide mixture injected into the channels. Since the goal was to culture mOECs with continuous chain-like structures it was hypothesized that reducing the channel diameter might drive the cell morphology towards spindle-like structures, characteristic of native bipolar OECs.[31,32] Additionally, for these multi-week experiments we selected the stiffest 15% w/v hydrogels as the channels in the softer hydrogels
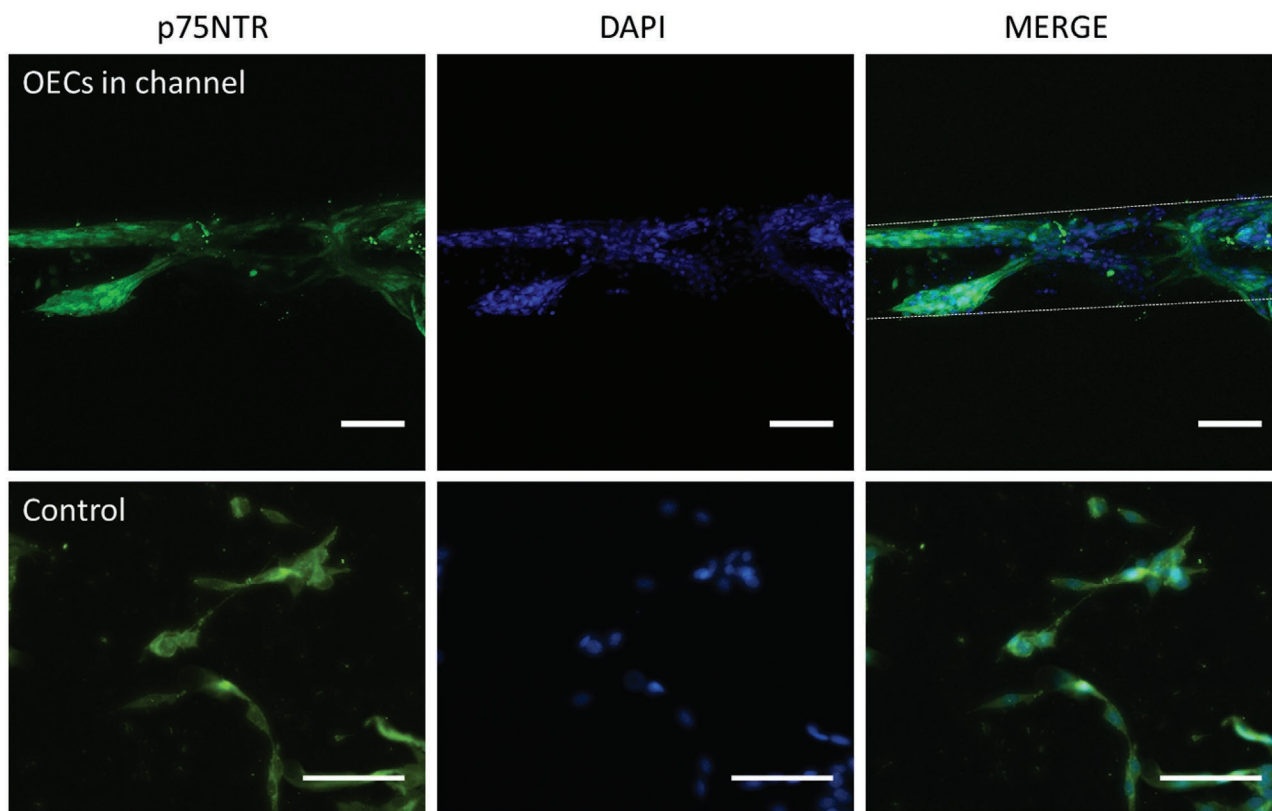
**ADVANCED
SCIENCE NEWS**
www.advancedsciencenews.com

**Macromolecular
Rapid Communications**
www.mrc-journal.de

Figure 3. mOECs cultured in 150 µm channels (top row) and on tissue culture plastic (bottom row) for 14 days and stained for p75NTR and DAPI. Scale bar = 100 µm.

closed in on themselves after 3–4 days of cell culture, possibly due to contractive forces from the cells.

Comparing the morphology of the mOECs in the three channel diameters after 14 days of culture (Figure S7, Supporting Information) showed the absence of cell spreading in the hydrogels without peptide regardless of channel diameter. For the hydrogels with peptide decorated channel walls OECs were adherent and exhibited spreading. The 300 µm diameter peptide patterned channels showed more chain-like formation by day 14 whereas the control without peptide did not promote cell adhesion or spreading. Further investigation of the influence of channel diameter involved observing the effect of 150 µm channels on cell behaviour. mOECs in 150 µm diameter channels patterned with peptide formed continuous chain-like structures by day seven which was faster than the larger channel diameters (Figure S7, Supporting Information). Upon higher magnification the mOECs also showed fine hairlike protrusions that contain parallel actin bundles (Figure S7c, Supporting Information). These extensions are one of the properties of OECs, and play a role in contact mediated migration,[33] characterized with substantial plasticity and capability to rapidly change morphology.[34]

For OECs to be useful for spinal cord injury treatment they need to express the typical markers characteristic of this lineage such as neurotrophin membrane receptor (p75NTR). The immunostaining of mOECs fixed on coverslips and in 150 µm diameter peptide patterned channels after culturing for 14 days showed that the cells stained positive for p75NTR (**Figure 3**). This confirmed that the mOECs that formed chain-like structures along the channels maintained their phenotype.

In summary, a facile hydrogel patterning approach was developed by injecting peptide solution in the channels produced from sacrificial molding. The diameters of the template were adjustable in the fabrication process and transferable to create channels in hydrogels. An adhesion peptide was conjugated to defined regions by the template with high fidelity and efficiency. The patterned channels were shown to support cell growth in a dose-dependent manner. In this study only one type of peptide was investigated, however, conceptually the same approach could be used with a range of peptides, including dual functionalization of both the channels and the bulk by sequential reaction of cysteine-peptide with the excess maleimide groups at the channel walls followed by reaction with the maleimide groups in the bulk of the hydrogels. In conclusion, this approach features the efficient use of peptide and the simplicity in manipulating physical and chemical characteristics, which facilitate powerful control in engineering tunable properties to study cell-substrate interactions within 3D cell culture experiments.

Experimental Section

Materials: Poly(ethylene glycol) of varying molecular weights were obtained from Jenkem Technology Co., Ltd., China. 4-arm PEG

maleimide (PEG-4Mal, M_w = 20000): ^{1}H NMR (600 MHz, CDCl$_3$)/ppm: δ 3.6 (m, −OCH$_2$−CH$_2$O−), 6.7 (s, CH$_2$ = CH$_2$). M_n estimated by ^{1}H NMR measurements was 22 560 g mol^{-1} and polydispersity was 1.1 as determined by size exclusion chromatography. 4-arm PEG thiol (PEG-4SH, M_w = 5000): ^{1}H NMR (600 MHz, CDCl$_3$)/ppm: δ 1.6 (t, 1H, −SH), 2.7 (q, 2H, −CH$_2$−SH), 3.6 (m, 152H, −OCH$_2$−CH$_2$O−). M_n 6820 g mol^{-1} and polydispersity 1.5. Peptide CRGDSGK (M_w = 721.8 g mol^{-1}) and fluorescein isothiocyanate (FITC)-tagged CRGDSGK (M_w = 1111.2 g mol^{-1}) were ordered from Pepmic Co., Ltd., China. Poly(ε-caprolactone) (PCL) filament (1.75 mm, M_n = 47500 g mol^{-1}, polydispersity = 1.8) for FDM was purchased from 3d4makers.com, the Netherlands. PCL pellet (Capa 6500C, M_w = 50000 g mol^{-1}) for MEW was sourced from Perstorp Ltd, UK. Gibco Dulbecco's Modified Eagle Medium (DMEM), fetal calf serum (FCS), L-glutamine 200 mm (100×), penicillin-streptomycin (Pen-Strep, 10000 U mL^{-1}), 0.05% trypsin-EDTA (1×), TrypLE (1×), and phosphate buffered saline (PBS) (0.01m) were sourced from ThermoFisher Scientific, USA.

Fabrication of PCL Structures Using FDM and MEW: PCL filament and scaffolds were printed using FDM with a FlashForge Dreamer 3D printer (FlashForge Corporation, Figure S1a, Supporting Information) with 0.2 mm aperture nozzle (Micro Swiss). Temperatures were set at 115 °C for extrusion and 30 °C for the platform. The printed parts were collected on aluminum foil taped to the platform. Different PCL filament diameters were obtained by adjusting the nozzle travel speed from 500 to 3000 mm min^{-1} with 500 mm min^{-1} intervals (Figure S2a, Supporting Information). 2D and 3D structures were designed using Autodesk CAD software and the G-codes were generated using Simplify3D software.

For MEW, a custom-built machine (Figure S1b, Supporting Information) was used as previous described.[27] A flat-tipped 21G nozzle, temperatures of 90 °C for the syringe and 95 °C for the nozzle were used. The PCL melt was MEW-processed using an applied voltage (+5 kV) and air pressure (4 bar) to extrude the polymer onto a collector at a distance of 6 mm from the nozzle, producing a range of filament diameters from 50 to 225 µm. Linear PCL filaments of different diameters were obtained by adjusting the collector speed assigned to each fibrous line from 60 to 600 mm min^{-1} with 60 mm min^{-1} intervals (Figure S2b, Supporting Information). In order to facilitate easy transfer and encapsulation of the PCL templates, MEW fibers were collected onto glass coverslips.

Preparation and Characterization of the Hydrogel: Fresh solutions of 14 mm PEG-4Mal and 21 mm PEG-4SH were prepared in sodium acetate/acetic acid buffer (pH = 4) before use. PEG-4Mal and PEG-4SH were mixed at a molar ratio of 1.5:1 and topped up with the buffer to reach solid contents (w/v) of 5%, 10%, and 15%. The precursors were briefly vortexed, centrifuged, and quickly dispensed around PCL templates (filament or scaffold) hung between two spacers on a hydrophobic glass slide pre-treated with Sigmacote (Merck). A hydrophobic glass coverslip pre-treated with Sigmacote was placed on the spacer, forming a round disk of polymer solution between the slides. Gelation was allowed to proceed in a humidified chamber for 30 min. Swelling ratios of the cured hydrogels were determined by immersing them in ddH$_2$O at room temperature (RT) for 24 h to reach equilibrium swelling (m_{sw}), and then dried to constant weight at 60 °C in the oven (m_{dry}). The mass swelling ratio (Q) and water content were calculated using the following equations:

$$Q = (m_{sw} - m_{dry}) / m_{dry} \tag{1}$$

$$\text{Water content}(\%) = 100 \times (m_{sw} - m_{dry}) / m_{sw} \tag{2}$$

The cured gel further swelled in water and the swelling after gelation was calculated using the equation:

$$\text{Gel swelling after gelation} = 100 \times (m_{sw(final)} - m_i) / m_i \tag{3}$$

where $m_{sw(final)}$ is the final swollen mass and m_i is the mass of water in the precursor solution.

Uniaxial compression was performed in air at 37 °C using an Instron universal testing system, fitted with a 5 kN load cell. The gel disk was compressed at a rate of 0.05 mm min^{-1}. Each sample was measured at least in triplicate.

Sacrificial Molding Process: After 30 min of gelation, the hydrogels encapsulating the linear PCL template were immersed in PBS causing gels to swell, allowing simple removal of the template. Complex PCL template structures were removed from the hydrogels by placing them in 90% acetone, followed by 20 min of ultra-sonication. Hydrogels with channels were soaked in PBS for 1 day before patterning with the peptide.

Peptide Patterning of the Hydrogels: First, a 10% (w/v, 138.5 mm) CRGDSGK peptide solution was prepared by dissolving in PBS. Then, FITC-tagged CRGDSGK (1 mg) was dissolved in DMSO (5.8 µL), followed by PBS (52.6 µL) to make a 15.4 mm stock solution. The peptide solutions were aliquoted (2 µL) and stored at −80 °C until use. 1 mm peptide mixtures of CRGDSGK and FITC-tagged CRGDSGK (molar ratio 9:1) were prepared by mixing 2 µL of each of the stock solutions in 304 µL of PBS.

To conjugate the peptide throughout the hydrogel, PEG-4Mal was first mixed with the CRGDSGK peptide and allowed to react for 1 h before PEG-4SH was added to form a gel. Ellman's test was performed to monitor the consumption of thiols in the PEG-4Mal and peptide mixture (thiols not detectable after 10 min).

To make peptide patterned channels, a 1 mm peptide mixture was injected into the channel using an ultrafine needle, and left in a humidified, dark chamber for 30 min. The perfusing peptide mixture was pipetted from the channel and its fluorescence intensity and residual thiol groups were measured. The gels were washed extensively with PBS and stored in the dark.

Fluorescence Readings and Imaging of Hydrogels: Fluorescence readings were obtained by using a POLARstar OPTIMA Microplate Reader (BMG Labtech, Germany) with 488/525 nm excitation/emission of FITC. A serial dilution of the solutions was made as peptide mixture standards, and the fluorescence intensity versus the concentration used to obtain the concentration of the peptide mixture after the hydrogel channels were perfused. Ellman's reagent was used to quantify free thiols in solution. The standard curve of the peptide mixture was linear in the range 10–200 µm and used to quantify the percentage residual thiols of the peptide mixture after conjugation via fluid flow.

Fluorescent and phase contrast images of the patterned hydrogels with and without the peptide were obtained using a Nikon SMZ25 fluorescence stereomicroscope (Nikon, Japan). Additionally, confocal laser scanning microscope images (CLSMs) of the patterned hydrogels were obtained using a Nikon A1R confocal microscope (Nikon, Japan).

Cell Culture: NIH-3T3 cells (passage 23–28) were cultured in DMEM medium supplemented with 1% Pen-Strep solution, 1% L-glutamine solution and 5% FCS at 37 °C and 5% CO$_2$. Mouse OECs were prepared as previously described.[35] mOECs (passage 11) were cultured in DMEM/F12 medium supplemented with 10% FBS and 1% Pen-Strep at 37 °C and 5% CO$_2$. For both cell types, the media was changed every 3 days and the cells passaged when 80% confluency was reached.

Hydrogels were sterilized by soaking in 80% ethanol for 30 min. After thorough washing with sterile PBS, the hydrogels were soaked in either NIH-3T3 or OEC cell culture medium. The hydrogels were allowed to acclimatize in the media for at least 24 h at 37 °C and 5% CO$_2$ prior to cell seeding.

NIH-3T3 cells and mOECs were harvested using trypsin or TrypLE, respectively. Cell numbers and viability were determined to achieve the desired cell seeding density of 400 cells mm^{-2} channel surface area. Hydrogel channels were seeded with either NIH-3T3 cells or mOECs with 5 µL of culture medium added to the bottom and top of each gel and left undisturbed for 3 h to allow cell attachment. The medium was then topped up to 1 mL, and changed every 2 or 3 days. Phase contrast images of the cell-laden patterned hydrogels with and without the peptide were obtained using a Nikon SMZ25 stereomicroscope.

Cell Staining and Imaging: Hydrogels containing NIH-3T3 cells were fixed with 4% paraformaldehyde (PFA) for 45 min at RT on day 7 and 14;

OECs were fixed on day 14. Following fixation, the hydrogels were washed using PBS, permeabilized with 0.1% TritonX-100 (Merck) for 1 h, and blocked overnight at 4 °C in 3% bovine serum albumin (BSA, Merck). Hydrogels containing OECs were incubated with the primary antibody p75NTR (1:100, Cat#839 701, BioLegend) and reconstituted in cold 3% BSA. Hydrogels containing NIH-3T3 cells were incubated in Alexa Fluor 488 conjugated Phalloidin (1:1000, Cat# A12379, ThermoFisher). Following primary antibody incubation, hydrogels containing mOECs were washed with PBS and incubated for 1 h at room temperature in the dark with appropriate Alexa Fluor conjugated secondary antibodies (1:200, Alexa Fluor 488, and Alexa Fluor 568, ThermoFisher). All hydrogels were counter-stained with DAPI (1:500, Cat# D1306, ThermoFisher), and imaged using a Nikon A1R confocal microscope.

Supporting Information

Supporting Information is available from the Wiley Online Library or from the author.

Acknowledgements

Conflict of Interest

The authors declare no conflict of interest.

Keywords

[1] P. D. Dalton, J. Mey, *Front. Biosci.* **2009**, *14*, 769.
[2] P. Musoke-Zawedde, M. S. Shoichet, *Biomed. Mater.* **2006**, *1*, 162.
[3] Y. Luo, M. S. Shoichet, *Nat. Mater.* **2004**, *3*, 249.
[4] S. Stokols, J. Sakamoto, C. Breckon, T. Holt, J. Weiss, M. H. Tuszynski, *Tissue Eng.* **2006**, *12*, 2777.
[5] P. D. Dalton, C. Hostert, K. Albrecht, M. Moeller, J. Groll, *Macromol. Biosci.* **2008**, *8*, 923.
[6] T. T. Yu, M. S. Shoichet, *Biomaterials* **2005**, *26*, 1507.
[7] L. Flynn, P. D. Dalton, M. S. Shoichet, *Biomaterials* **2003**, *24*, 4265.
[8] K. S. Lim, M. Baptista, S. Moon, T. B. F. Woodfield, J. Rnjak-Kovacina, *Trends Biotechnol.* **2019**, *37*, 1189.
[9] J. S. Miller, K. R. Stevens, M. T. Yang, B. M. Baker, D.-H. T. Nguyen, D. M. Cohen, E. Toro, A. A. Chen, P. A. Galie, X. Yu, R. Chaturvedi, S. N. Bhatia, C. S. Chen, *Nat. Mater.* **2012**, *11*, 768.
[10] J. N. Haigh, Y.-M. Chuang, B. Farrugia, R. Hoogenboom, P. D. Dalton, T. R. Dargaville, *Macromol. Rapid Commun.* **2016**, *37*, 93.
[11] K. H. Song, C. B. Highley, A. Rouff, J. A. Burdick, *Adv. Funct. Mater.* **2018**, *28*, 1801331.
[12] L. E. Bertassoni, M. Cecconi, V. Manoharan, M. Nikkhah, J. Hjortnaes, A. L. Cristino, B. Barabaschi, D. Demarchi, M. R. Dokmeci, Y. Yang, A. Khademhosseini, *Lab Chip* **2014**, *14*, 2202.
[13] V. K. Lee, D. Y. Kim, H. Ngo, Y. Lee, L. Seo, S.-S. Yoo, P. A. Vincent, G. Dai, *Biomaterials* **2014**, *35*, 8092.
[14] D. B. Kolesky, R. L. Truby, A. S. Gladman, T. A. Busbee, K. A. Homan, J. A. Lewis, *Adv. Mater.* **2014**, *26*, 3124.
[15] J. B. Lee, X. Wang, S. Faley, B. Baer, D. A. Balikov, H.-J. Sung, L. M. Bellan, *Adv. Healthcare Mater.* **2016**, *5*, 781.
[16] K. Pataky, M. Ackermann, T. Braschler, M. Lutolf, P. Renaud, J. Brugger, Int. Conf. on Digital Printing Technologies, Society for Imaging Science and Technology, Arlington, VA, USA **2009**, p. 411.
[17] A. Ranga, S. Gobaa, Y. Okawa, K. Mosiewicz, A. Negro, M. P. Lutolf, *Nat. Commun.* **2014**, *5*, 4324.
[18] N. Huettner, T. R. Dargaville, A. Forget, *Trends Biotechnol.* **2018**, *36*, 372.
[19] S. Wang, P. D. Dalton, T. R. Dargaville, *Macromol. Rapid Commun.* **2018**, *39*, 1800635.
[20] M. Oudega, *Acta Physiol.* **2007**, *189*, 181.
[21] P. D. Dalton, C. Vaquette, B. L. Farrugia, T. R. Dargaville, T. D. Brown, D. W. Hutmacher, *Biomater. Sci.* **2013**, *1*, 171.
[22] T. D. Brown, P. D. Dalton, D. W. Hutmacher, *Prog. Polym. Sci.* **2016**, *56*, 116.
[23] G. Hochleitner, J. F. Hümmer, R. Luxenhofer, J. Groll, *Polymer* **2014**, *55*, 5017.
[24] G. Hochleitner, T. Jüngst, T. D. Brown, K. Hahn, C. Moseke, F. Jakob, P. D. Dalton, J. Groll, *Biofabrication* **2015**, *7*, 035002.
[25] O. Bas, E. M. De-Juan-Pardo, M. P. Chhaya, F. M. Wunner, J. E. Jeon, T. J. Klein, D. W. Hutmacher, *Eur. Polym. J.* **2015**, *72*, 451.
[26] F. M. Wunner, O. Bas, N. T. Saidy, P. D. Dalton, E. M. D.-J. Pardo, D. W. Hutmacher, *J. Visualized Exp.* **2017**, *130*, e56289.
[27] T. D. Brown, P. D. Dalton, D. W. Hutmacher, *Adv. Mater.* **2011**, *23*, 5651.
[28] P. M. Kharkar, R. A. Scott, L. P. Olney, P. J. LeValley, E. Maverakis, K. L. Kiick, A. M. Kloxin, *Adv. Healthcare Mater.* **2017**, *6*, 1700713.
[29] L. E. Jansen, L. J. Negrón-Piñeiro, S. Galarza, S. R. Peyton, *Acta Biomater.* **2018**, *70*, 120.
[30] K. Bott, Z. Upton, K. Schrobback, M. Ehrbar, J. A. Hubbell, M. P. Lutolf, S. C. Rizzi, *Biomaterials* **2010**, *31*, 8454.
[31] J. R. Higginson, S. C. Barnett, *Exp. Neurol.* **2011**, *229*, 2.
[32] Z. H. Huang, Y. Wang, L. Cao, Z. D. Su, Y. L. Zhu, Y. Z. Chen, X. B. Yuan, C. He, *Cell Res.* **2008**, *18*, 479.
[33] D. A. Knecht, F. Xue, D. M. Janzen, *Int. J. Cell Biol.* **2010**, *2010*, 507821.
[34] A. N. Van Den Pol, J. G. Santarelli, *J. Comp. Neurol.* **2003**, *458*, 175.
[35] J. T. Velasquez, M. E. Watts, M. Todorovic, L. Nazareth, E. Pastrana, J. Diaz-Nido, F. Lim, J. A. K. Ekberg, R. J. Quinn, J. A. St John, *PLoS One* **2014**, *9*, e87732.